Synthesis and crystal structures of $[H_3N(CH_2)_2NH_3]NbMOF(PO_4)_2(H_2O)_2$, M = Fe,Co and $[H_3N(CH_2)_2NH_3]Ti(Fe_{0.9}Cr_{0.1})(F_{1.3}O_{0.7})(H_{0.3}PO_4)_2(H_2O)_2$

Xiqu Wang, Lumei Liu, Heidi Cheng, Kent Ross and Allan J. Jacobson*

*Department of Chemistry, University of Houston, Houston, Texas, 77204-5641, USA;
E-mail: ajjacob@uh.edu*

The new niobium phosphates $[H_3N(CH_2)_2NH_3]NbFeOF(PO_4)_2(H_2O)_2$ and $[H_3N(CH_2)_2NH_3]NbCoOF(PO_4)_2(H_2O)_2$ have been synthesized in single crystal form by hydrothermal reactions at 165 °C. The new phase $[H_3N(CH_2)_2NH_3]Ti(Fe_{0.9}Cr_{0.1})(F_{1.3}O_{0.7})(H_{0.3}PO_4)_2(H_2O)_2$ has been obtained by hydrothermal electrocrystallization at 170 °C. The crystal structures have been refined from X-ray diffraction data. They are structurally similar to the known layered iron phosphate $[H_3N(CH_2)_2NH_2][Fe_2F_2(HPO_4)_2(H_2O)_2]$ designated as ULM-10 and the mineral curetonite.

Introduction

Open framework phosphates have been widely investigated since the discovery of a group of microporous aluminophosphates in the early eighties.[1] Subsequent synthesis approaches were successful in replacing the aluminium with other metals.[2–9] In particular, incorporation of transition metal elements may lead to microporous materials with interesting electrical and magnetic properties.[9] Recently, a number of fluorometallophosphates with open-framework structures have been reported, mainly by Férey and co-workers.[4,9–15] These compounds were hydrothermally synthesized in the systems M–P–F–amine–H_2O with M = Al, Ga, Fe, V and Ti. Hydrothermal syntheses of niobium phosphates are rare but some alkali metal niobium phosphates have been previously synthesized hydrothermally at rather high temperatures (>600 °C).[16]

We have synthesized several novel compounds including metal phosphates by electrochemical oxidation of a metal electrode under hydrothermal conditions.[17,18] In comparison studies, we found that the syntheses in the presence (electrochemical–hydrothermal) and absence (hydrothermal) of an applied electric potential often led to different products. Well developed single crystals of complex compounds could be obtained in both cases, indicating that the two methods are complementary and both are effective for exploratory synthesis of new materials. Here we report the novel layered phosphates $[H_3N(CH_2)_2NH_3]NbFeOF(PO_4)_2(H_2O)_2$ (**1**) and $[H_3N(CH_2)_2NH_3]NbCoOF(PO_4)_2(H_2O)_2$ (**2**) synthesized hydrothermally and $[H_3N(CH_2)_2NH_3]Ti(Fe_{0.9}Cr_{0.1})(F_{1.3}O_{0.7})(H_{0.3}PO_4)_2(H_2O)_2$ (**3**) obtained by the electrochemical–hydrothermal method.

Experimental

Synthesis

In a typical synthesis of compound **1**, a solution was prepared by dissolving 0.085 ml phosphoric acid and 43 mg NH_4HF_2 in 2.1 ml H_2O. The solution was mixed with 0.05 ml ethylenediamine, and then sealed together with 15 mg niobium and 1.5 mg iron metal in a flexible Teflon bag in air. The bag was subsequently sealed in a steel reaction vessel filled with water to about 60% volume, and heated at 165 °C for 38 h. The products were washed with water, filtered and dried in air. Compound **2** was similarly synthesized by replacing iron metal in the starting material with cobalt metal.

Compound **3** was obtained in an experiment in which titanium was introduced to the reaction electrochemically. A solution of 2.0 ml phosphoric acid, 2.9 g KHF_2 and 1.0 ml ethylenediamine in 40 ml water (pH = 4.1) was transferred to an open Teflon container and sealed in a Parr autoclave (inner volume: 100 ml) fitted with feedthroughs for electrical connections between the electrodes inside the reaction chamber and the external circuit. The anode (working electrode) was a titanium metal plate ($20 \times 10 \times 0.254$ mm). A gold foil was used as cathode (counter electrode). The experiment was conducted with a current density of *ca.* 1 mA cm^{-2} generated by a commercial power source (MacPile, Biologic Scientific Instruments) at 170 ± 2 °C for 110 h. The pH after the reaction was 4.4.

Characterization

The chemical compositions were analyzed using a JEOL 8600 electron microprobe operating at 15 KeV with a 10 μm beam diameter and a beam current of 30 nA. Infrared spectra were collected with a Galaxy FTIR 5000 series spectrometer using the KBr pellet method. Thermogravimetric analyses were carried out with a heating rate of 10 °C min^{-1} in air, on a DuPont 2100 TGA system.

Single crystal X-ray data were measured on a SMART platform diffractometer equipped with a 1 K CCD area detector using graphite-monochromatized Mo-Kα radiation at 293 K.[19] Absorption correction was made using the program SADABS.[20] The structures were solved by direct methods and refined using SHELXTL.[21] All non-hydrogen positions were refined anisotropically in the final refinements. The hydrogen atoms were located from difference maps and refined isotropically with atom distance and angle constraints. Crystallographic and refinement details are summarized in Table 1. The final *R*-indices for **3** are moderately high probably because of the disorder and poor crystal quality. Atom positions are given in Table 2 and selected bond lengths and bond angles in Table 3.

CCDC reference number 1145/208. See http://www.rsc.org/suppdata/jm/a9/a909193i/ for crystallographic files in .cif format.

Table 1 Crystal and structure refinement data for [H$_3$N(CH$_2$)$_2$NH$_3$]NbFeOF(PO$_4$)$_2$(H$_2$O)$_2$ (**1**), [H$_3$N(CH$_2$)$_2$NH$_3$]NbCoOF(PO$_4$)$_2$(H$_2$O)$_2$ (**2**) and [H$_3$N(CH$_2$)$_2$NH$_3$]Ti(Fe$_{0.9}$Cr$_{0.1}$)(F$_{1.3}$O$_{0.7}$)(H$_{0.3}$PO$_4$)$_2$(H$_2$O)$_2$ (**3**)

	1	**2**	**3**
Formula	C$_2$H$_{14}$N$_2$O$_{11}$FFeNbP$_2$	C$_2$H$_{14}$N$_2$O$_{11}$FCoNbP$_2$	C$_2$H$_{14.3}$N$_2$O$_{10.7}$F$_{1.3}$Cr$_{0.1}$Fe$_{0.9}$TiP$_2$
M	471.85	474.93	427.49
Crystal size/mm	0.44 × 0.26 × 0.10	0.38 × 0.24 × 0.09	0.24 × 0.18 × 0.08
Temperature/K	293(2)	293(2)	293(2)
Wavelength/Å	0.71073	0.71073	0.71073
Space group	$P\bar{1}$	$P\bar{1}$	$P\bar{1}$
Unit cell dimensions:			
a/Å	5.0715(6)	5.0469(5)	5.158(1)
b/Å	7.529(1)	7.4870(8)	7.456(1)
c/Å	9.150(1)	9.122(1)	9.089(2)
α/°	72.441(3)	72.486(2)	63.87(3)
β/°	85.679(2)	85.679(2)	80.60(3)
γ/°	70.480(2)	70.800(2)	69.791(3)
Volume/Å^3, Z	313.80(7), 1	310.31(6), 1	294.5(1), 1
Absorption coeff./mm^{-1}	2.396	2.591	2.216
Reflections collected	1991	1949	1736
Independent reflections	1380	1356	1214
Data/parameters	1380/100	1356/100	1214/98
$R1$/$wR2$ for $I>2\sigma(I)$	0.0473/0.1131	0.0569/0.1325	0.0976/0.2103
$R1$/$wR2$ for all data^a	0.0490/0.1138	0.0599/0.1339	0.1548/0.2412

$^a R1 = \Sigma||F_o|-|F_c||/\Sigma|F_o|$. $wR2 = [\Sigma(w(F_o^2-F_c^2)^2)/\Sigma(wF_o^2)^2]^{1/2}$.

Results and discussion

Synthesis

Yellow platy crystals of compound **1** were recovered together with unreacted niobium metal. Pink plates of compound **2** formed together with colorless unidentified impurities and unreacted niobium metal. For both compounds the yields are less than 20% based on niobium. Efforts to improve the yields by varying the relative contents of phosphoric acid and amines, and Nb : M ratios in the reagents, were unsuccessful. Compound **2** can also be synthesized by using homopiperazine C$_5$H$_{12}$N$_2$ to replace ethylenediamine in the starting mixture.

Table 2 Atomic coordinates ($\times 10^4$) and equivalent isotropic displacement parameters (Å$^2 \times 10^3$). U(eq) is defined as one-third of the trace of the orthogonalized U_{ij} tensor

	x	y	z	U(eq)
[H$_3$N(CH$_2$)$_2$NH$_3$]NbFeOF(PO$_4$)$_2$(H$_2$O)$_2$ (**1**)				
Nb	5000	0	0	18(1)
P	880(2)	−2354(2)	2224(1)	10(1)
Fe	5000	5000	0	12(1)
O(1)	−2263(7)	−1591(6)	1751(4)	18(1)
O(2)	2347(8)	−4178(5)	1693(4)	19(1)
O(3)	2021(7)	−631(5)	1374(4)	15(1)
O(4)	1171(8)	−2807(6)	3936(4)	18(1)
O(5), F	4279(7)	2331(5)	650(4)	19(1)
N	4093(10)	−7256(7)	4616(5)	20(1)
C	4803(14)	−9166(8)	4268(6)	24(1)
OW	1499(9)	6332(7)	−1698(5)	26(1)
[H$_3$N(CH$_2$)$_2$NH$_3$]NbCoOF(PO$_4$)$_2$(H$_2$O)$_2$ (**2**)				
Nb	5000	0	0	16(1)
P	856(3)	−2350(2)	2233(2)	7(1)
Co	5000	5000	0	8(1)
O(1)	−2314(9)	−1603(7)	1763(5)	13(1)
O(2)	2317(10)	−4171(7)	1696(5)	15(1)
O(3)	1982(9)	−598(6)	1364(5)	12(1)
O(4)	1168(10)	−2805(7)	3943(5)	13(1)
O(5), F	4306(9)	2365(6)	630(5)	14(1)
N	4089(12)	−7243(8)	4588(7)	15(1)
C	4784(16)	−9163(10)	4256(8)	18(1)
OW	1559(10)	6293(7)	−1650(6)	17(1)
[H$_3$N(CH$_2$)$_2$NH$_3$]Ti(Fe$_{0.9}$Cr$_{0.1}$)(F$_{1.3}$O$_{0.7}$)(H$_{0.3}$PO$_4$)$_2$(H$_2$O)$_2$ (**3**)				
Ti	5000	0	0	22(1)
Fe, Cr	5000	5000	0	19(1)
P	699(5)	7346(4)	2257(4)	17(1)
O(1)	−2332(15)	8076(12)	1841(10)	26(2)
O(2)	2345(16)	5485(12)	1855(10)	29(2)
O(3)	1940(15)	9164(12)	1478(10)	25(2)
O(4)	787(16)	6565(12)	4146(10)	27(2)
O(5), F	4294(14)	2214(10)	679(9)	28(2)
OW	1460(16)	6592(14)	−1692(10)	32(2)
N	−4684(19)	12 419(14)	−5039(12)	28(2)
C	−3818(26)	10 260(21)	−4894(18)	37(3)

Table 3 Selected bond lengths (Å) and angles (°)

[H₃N(CH₂)₂NH₃]NbFeOF(PO₄)₂(H₂O)₂ (1)

$[H_3N(CH_2)_2NH_3]NbFeOF(PO_4)_2(H_2O)_2$ **(1)**

Nb–	Distance	Angles				
O5, F	1.933(3)					
O5, F	1.933(3)	180.00				
O3	1.981(3)	91.7(1)	88.3(1)			
O3	1.981(3)	88.3(1)	91.7(1)	180.00		
O1	1.999(4)	89.3(2)	90.7(2)	88.0(2)	92.0(2)	
O1	1.999(4)	90.7(2)	89.3(2)	92.0(2)	88.0(2)	180.00

Fe–						
O5, F	2.064(3)					
O5, F	2.064(3)	180.00				
O2	2.074(4)	89.1(1)	90.9(1)			
O2	2.074(4)	90.9(1)	89.1(1)	180.00		
Ow	2.204(4)	88.3(2)	91.7(2)	88.9(2)	91.1(2)	
Ow	2.204(4)	91.7(2)	88.3(2)	91.1(2)	88.9(2)	180.00

P–				
O4	1.507(4)			
O2	1.530(4)	111.7(2)		
O1	1.549(4)	109.4(2)	108.7(2)	
O3	1.565(4)	110.5(2)	110.8(2)	105.5(2)

[H₃N(CH₂)₂NH₃]NbFeOF(PO₄)₂(H₂O)₂ (2)

$[H_3N(CH_2)_2NH_3]NbFeOF(PO_4)_2(H_2O)_2$ **(2)**

Nb–	Distance	Angles				
O5, F	1.940(4)					
O5, F	1.940(4)	180.00				
O3	1.974(4)	91.6(2)	88.4(2)			
O3	1.974(4)	88.4(2)	91.6(2)	180.00		
O1	1.990(4)	91.2(2)	88.8(2)	92.2(2)	87.8(2)	
O1	1.990(4)	88.8(2)	91.2(2)	87.8(2)	92.2(2)	180.00

Co–						
O5, F	2.021(4)					
O5, F	2.021(4)	180.00				
O2	2.079(5)	90.5(2)	89.5(2)			
O2	2.079(5)	89.5(2)	90.5(2)	180.00		
OW	2.151(5)	91.7(2)	88.3(2)	89.5(2)	90.5(2)	
OW	2.151(5)	88.3(2)	91.7(2)	90.5(2)	89.5(2)	180.00

P–				
O4	1.502(5)			
O2	1.526(5)	111.6(3)		
O1	1.558(5)	109.7(3)	108.4(3)	
O3	1.571(5)	110.8(3)	110.8(3)	105.3(3)

[H₃N(CH₂)₂NH₃]Ti(Fe₀.₉Cr₀.₁)(F₁.₃O₀.₇)(H₀.₃PO₄)₂(H₂O)₂ (3)

$[H_3N(CH_2)_2NH_3]Ti(Fe_{0.9}Cr_{0.1})(F_{1.3}O_{0.7})(H_{0.3}PO_4)_2(H_2O)_2$ **(3)**

Ti–	Distance	Angles				
O5, F	1.910(6)					
O5, F	1.910(6)	180.00				
O3	1.983(7)	91.8(3)	88.2(3)			
O3	1.983(7)	88.2(3)	91.8(3)	180.00		
O1	2.006(8)	90.1(3)	89.9(3)	90.3(3)	89.8(3)	
O1	2.006(8)	89.9(3)	90.1(3)	89.8(3)	90.3(3)	180.00

Fe, Cr–						
O5, F	2.037(6)					
O5, F	2.037(6)	180.00				
O2	2.071(7)	90.6(3)	89.4(3)			
O2	2.071(7)	89.4(3)	90.6(3)	180.00		
OW	2.218(9)	89.4(3)	90.6(3)	90.3(3)	89.7(3)	
OW	2.218(9)	90.6(3)	89.4(3)	89.7(3)	90.3(3)	180.00

P–				
O1	1.519(8)			
O2	1.520(7)	111.6(5)		
O3	1.534(8)	111.7(4)	113.0(4)	
O4	1.555(9)	105.9(4)	107.1(5)	107.1(5)

During reaction the homopiperazine molecules were cleaved to form protonated ethylenediammonium cations. This reaction and the subsequent incorporation of enH₂ in **2** was confirmed by single crystal structure refinements and IR spectra. Electrochemical–hydrothermal syntheses of **1** and **2** by using a niobium anode under conditions similar to the synthesis of **3** were unsuccessful.

Light brown plates of compound **3** were formed on the titanium electrode in the electrochemical–hydrothermal experiment. The Fe and Cr in the compound arise from reactions with the autoclave cap that was made of T316 stainless steel. The yield is about 5% based on titanium. Attempts to synthesize compound **3** hydrothermally by using Ti, Fe and Cr metals were not successful.
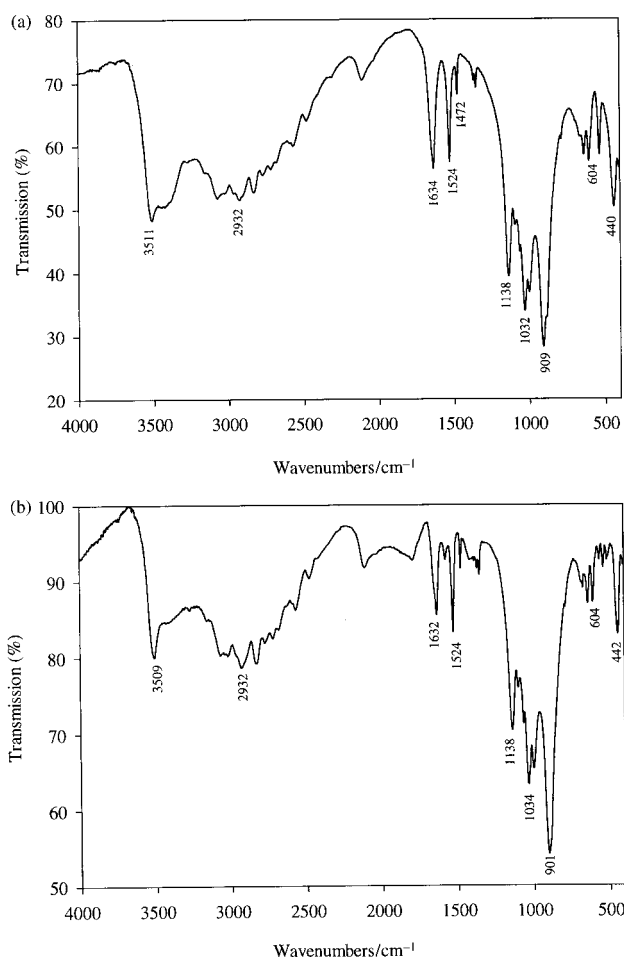
Characterization

The electron microprobe measurements gave atomic ratios: $Nb:Fe:P:F = 1:0.99:1.97:0.84$ for **1**, $Nb:Co:P:F = 1:0.98:2.05:0.85$ for **2**, and $Ti:Fe:Cr:P:F = 1:0.86:0.13:2.04:1.33$ for **3**, which are reasonably consistent with the formula ratios derived from the structure refinements.

Fig. 1 shows the infrared spectra of the compounds **1** and **2**. Characteristic bands for protonated ethylenediamine (2500–3100, 1472, 1524 cm^{-1}) and water molecules are observed (ca. 1634 and ca. 3400–3510 cm^{-1}). The bands between 901 and 1138 cm^{-1} are typical for stretching of phosphate anions. The isostructural relationship of the two compounds is clearly reflected in the similarity of the spectra. In fact, identical orientations of the $H_3N(CH_2)_2NH_3$ cations with respect to the other parts of the structures in **1** and **2** were revealed by the structure refinements.

Thermogravimetric analysis was carried out for $[H_3N(CH_2)_2NH_3]NbCoOF(PO_4)_2(H_2O)_2$ (**2**) as a representative example. The data (Fig. 2) show a single weight loss that began at ca. 280 °C and was completed at ca. 500 °C. The observed weight loss of 24.2% is consistent with the theoretical value of 24.0% calculated by assuming that the final product is $NbCo(PO_4)_2F$.

Crystal structures

The structures of the three compounds consist of metal phosphate layers and interlayer $H_3N(CH_2)_2NH_3$ cations. The layers are topologically the same as those in the known iron phosphate $[H_3N(CH_2)_2NH_2][Fe_2F_2(HPO_4)_2(H_2O)_2]$ designated

as ULM-10[10] and the mineral curetonite $Ba_2[(Al,Ti)Al(OH,O)_2(PO_4)_2F_2]$.[22]

Fig. 3a shows the coordination environments of the metal atoms in the structure of **1**. Both Nb and Fe atoms are on a symmetry center and have octahedral coordination. The Nb atom is coordinated by four oxygen atoms in the equatorial plane. The two apical corners of the octahedron are randomly occupied by a fluorine and an oxygen atom. The Fe atom has a similar coordination environment but has two water oxygen atoms in *trans* positions. A bond valence sum calculated with empirical parameters[23] indicated that Fe is divalent (2.09 v.u.). The NbO_5F and FeO_5F octahedra are linked into infinite chains along [010] by sharing the apical F and O atoms. The octahedral chains are interconnected by the PO_4 tetrahedra into layers parallel to the (001) plane (Fig. 4). Each PO_4

Fig. 3 The local coordination environments of cations (a) in compound **1** and (b) in compound **3**. Thermal ellipsoids are plotted with 50% probability.


Fig. 1 IR spectra of (a) $[H_3N(CH_2)_2NH_3]NbFeOF(PO_4)_2(H_2O)_2$, **1**; (b) $[H_3N(CH_2)_2NH_3]NbCoOF(PO_4)_2(H_2O)_2$, **2**.
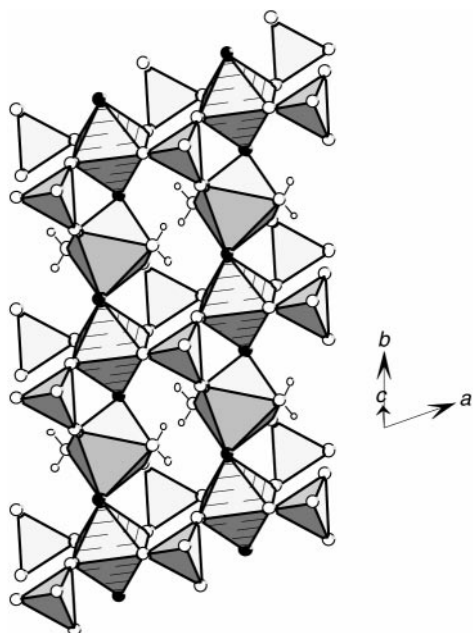
Fig. 4 A view of the metal phosphate layer in compound **1**. NbO_5F octahedra are hatched. Solid circles are positions randomly occupied by O and F atoms.

tetrahedron shares corners with a NbO_5F and a FeO_5F octahedron from the same chain and a NbO_5F octahedron from a neighboring chain. Thus the NbO_5F octahedron is linked with four PO_4 tetrahedra while the FeO_5F octahedron is linked with two tetrahedra. The layers are stacked along [001] with $[H_3N(CH_2)_2NH_3]^{2+}$ cations occupying interlayer spaces (Fig. 5). The compound **2** is isostructural with **1**. The bond valence sum calculated for Co is 2.05 v.u. which is consistent with the expected divalent character of cobalt in **2**.

In the structure refinements each apical corner of the octahedra was assumed to be randomly occupied by a fluorine or an oxygen atom. This is because both the Nb and the Fe/Co atoms are located at special positions in the space group $P\bar{1}$. If the structure is ordered, the backbone of the octahedral chains can be (i) O–Nb–F–M–O–Nb–F or (ii) O–Nb–F–M–F–Nb–O–M–O–Nb–F–M–F. Case (i) requires breaking of the inversion symmetry while case (ii) needs a doubling of the unit cell dimension along the b axis. Superstructure reflections corresponding to the cell doubling were not detected by using extended exposure time. Refinements with models corresponding to both cases resulted in unreasonably large correlation matrix elements and atom positions with non-positive definite thermal parameters, and therefore were unsuccessful. However, the possibility that the structure is actually ordered can not be ruled out because of the similarity in X-ray scattering power of F and O. The disordered structure given here represents full disorder of the local cases (i) and (ii). The strongly elongated thermal ellipsoids of the Nb atoms shown in Fig. 3a result from averaging local F–Nb–O and O–Nb–F bonds. The apical Nb–O bond is expected to be shorter than the Nb–F bond.

The metal phosphate layers in **3** are structurally the same as those in **1** and **2**. However, the orientations of the interlayer $[H_3N(CH_2)_2NH_3]^{2+}$ cations are substantially different. In the structures of **3** and ULM-10, the N–C–C–N bonds are in a plane that is roughly parallel to the phosphate layers (Fig. 5b). In contrast, the corresponding N–C–C–N plane in the structures of **1** and **2** is almost perpendicular to the phosphate layers (Fig. 5a). This orientation change can be understood from the requirements of hydrogen bonding between the $[H_3N(CH_2)_2NH_3]^{2+}$ cations and the layer oxygen atoms. In the structure of **3** the –NH_3 group forms hydrogen bonds with the
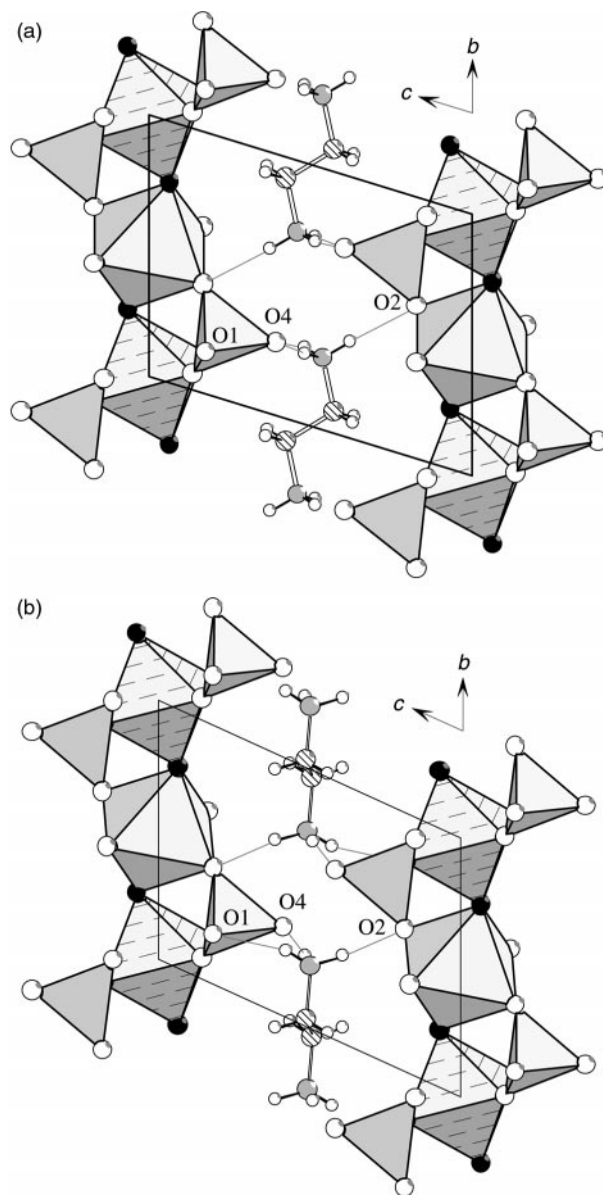
Fig. 5 Comparison of the structures of (a) **1**; and (b) **3**.

O1, O2 and O4 atoms. ($d_{(N–O1)} = 3.00$ Å, $d_{(H3–O1)} = 2.11$ Å; $d_{(N–O2)} = 2.98$ Å, $d_{(H1–O2)} = 2.04$ Å; $d_{(N–O4)} = 2.71$ Å, $d_{(H2–O4)} = 1.77$ Å). The O1 atom is bonded to a P^{5+} and a Ti^{4+} cation and has a bond valence sum of 1.85 v.u. The corresponding O1 atom in the structure of **1** is bonded to a P^{5+} and a Nb^{5+} cation and has a saturated bond valence sum of 1.95 v.u (1.94 v.u. in compound **2**) apparently because of the high valence of the niobium cation. Therefore, the O1 atoms in **1** and **2** are not suitable as hydrogen bond acceptors. By adjusting the orientation of the $[H_3N(CH_2)_2NH_3]^{2+}$ cation, the –NH_3 group in **1** and **2** forms hydrogen bonds with an O2 atom that bridges a P^{5+} and a divalent metal cation, and two terminal O4 atoms of the phosphate tetrahedra (in compounds **1**/**2**: $d_{(N–O2)} = 2.93/2.90$ Å, $d_{(H3–O2)} = 2.05/2.02$ Å; $d_{(N–O4)} = 2.85/2.85$ Å, $d_{(H2–O4)} = 1.97/1.96$ Å; $d_{(N–O4)} = 2.88/2.88$ Å, $d_{(H1–O4)} = 2.02/2.02$ Å). The valence difference between the niobium and titanium cations also has considerable effects on the phosphate tetrahedra. In **1** and **2** the P–O1 and P–O3 bonds are weaker than in **3** because of the stronger Nb–O1 and Nb–O3 bonds. As a consequence, the terminal P–O4 bonds are much shorter in **1** and **2** than in **3**. In fact, the O4 atoms in **3** are partially protonated, *i.e.*, part of the phosphate anions should be HPO_4 groups ($\sim 30\%$). The partial protonation is also in agreement with the fact that the averaged O4–P–O bond angle

in **3** (106.7°) is smaller than in **1** and **2** (110.6°) because a decrease in double bond character of the P–O4 bond would decrease this angle. In [H$_3$N(CH$_2$)$_2$NH$_2$][Fe$_2$F$_2$(HPO$_4$)$_2$(H$_2$O)$_2$] (ULM-10), the corresponding terminal oxygen position is occupied by a hydroxyl group, and neighboring phosphate layers are linked by hydrogen bonds between the hydroxyl groups.

Conclusions

Hydrothermal reactions at 165 °C resulted in the new niobium phosphates **1** and **2** in single crystal forms. The new titanium phosphate **3** has been obtained by hydrothermal electrocrystallization at 170 °C. The compounds **1–3** are structurally similar to the known iron phosphate ULM-10. Different orientations of the [H$_3$N(CH$_2$)$_2$NH$_3$]$^{2+}$ cations in these compounds are due to hydrogen bonding requirements. The low temperature synthesis route using niobium metal and HF$_2^-$ as a mineralizer has general applicability. We have obtained a number of other novel niobium phosphates in single crystal form by using this technique.[24]

References

1 S. T. Wilson, B. M. Lok, C. A. Messina, T. R. Cannan and E. M. Flanigen, *J. Am. Chem. Soc.*, 1982, **104**, 1146.

2 R. C. Haushalter, K. G. Strohmaier and F. W. Lai, *Science*, 1989, **246**, 1289.

3 A. Merrouche, J. Patrarin, H. Kessler, M. Soulard, L. Delmotte, J. L. Guth and J. F. Joly, *Zeolites*, 1992, **12**, 226.

4 G. Férey, *J. Fluorine Chem.*, 1995, **72**, 187.

5 M. I. Khan, L. M. Meyer, R. C. Haushalter, A. L. Schweizer, J. Zubieta and J. I. Dye, *Chem. Mater.*, 1996, **8**, 43.

6 L. M. Meyer, R. C. Haushalter and J. Zubieta, *J. Solid State Chem.*, 1996, **125**, 200.

7 P. Feng, X. Bu and G. Stucky, *Nature*, 1997, **388**, 735.

8 K.-H. Lii, Y.-F. Huang, V. Zima, C.-Y. Huang, H.-M. Lin, Y.-C. Jiang, F.-l. Liao and S.-L. Wang, *Chem. Mater.*, 1998, **10**, 2599.

9 M. Cavellec, D. Riou and G. Férey, *Inorg. Chim. Acta*, 1999, **291**, 317.

10 M. Cavellec, D. Riou and G. Férey, *J. Solid State Chem.*, 1994, **112**, 441.

11 D. Riou and G. Férey, *J. Mater. Chem.*, 1998, **8**, 2733.

12 F. Taulelle, A. Samoson and G. Férey, *J. Phys. Chem.*, 1998, **102**, 8588.

13 N. Simon, T. Loiseau and G. Férey, *J. Mater. Chem.*, 1999, **9**, 585.

14 C. Serre and G. Férey, *J. Mater. Chem.*, 1999, **9**, 579.

15 C. Serre, N. Guillou and G. Férey, *J. Mater. Chem.*, 1999, **9**, 1185.

16 C. S. Liang, W. T. A. Harrison, M. M. Eddy, T. E. Gier and G. Stucky, *Chem. Mater.*, 1993, **5**, 917.

17 X. Wang, L. Liu, A. J. Jacobson and K. Ross, *J. Mater. Chem.*, 1999, **9**, 859.

18 L. Liu, X. Wang, R. Bontchev, K. Ross and A. J. Jacobson, *J. Mater. Chem.*, 1999, **9**, 1585.

19 SAINT, Program for Data Extraction and Reduction, Siemens Analytical X-ray Instruments Inc., Madison, USA, 1994–1996.

20 G. M. Sheldrick, SADABS, Program for Siemens Area Detector Absorption Corrections, University of Gottingen, Germany, 1997.

21 G. M. Sheldrick, SHELXTL, Program for Refinement of Crystal Structures, Siemens Analytical X-ray Instruments Inc., Madison, USA, 1994.

22 M. Cooper and F. C. Hawthorne, *Am. Mineral.*, 1994, **79**, 545.

23 N. Brese and M. O'Keeffe, *Acta Crystallogr., Sect. B*, 1991, **47**, 192.

24 X. Wang, L. Liu, H. Cheng and A. J. Jacobson, *Chem. Commun.*, 1999, 2531.